



Engineered Oncolytic Virus for the Treatment of Cholesteatoma: A Pilot in vivo Study

Ravi N. Samy, MD, FACS ; Brian R. Earl, PhD; Noga Lipschitz, MD ; Ivy Schweinzger, BS; Mark Currier, MS; Timothy Cripe, MD, PhD

Objective: Determine if oncolytic herpes simplex virus (oHSV) can eradicate cholesteatoma (CHST) in a gerbil model.

Methods: An in vivo model of CHST was developed in Mongolian gerbils by combining *Pseudomonas aeruginosa* inoculation with double ligation of the external auditory canal (EAC). CHST size and bone thickness were measured using morphometric and volumetric quantification techniques via micro-computed tomography (micro-CT). The CHST induction and quantification techniques were then used in an additional group of 10 gerbils ($n = 20$ ears) to determine the within-group treatment efficacy of oHSV against CHST in vivo. Treated animals received either one, two, or three intrabullar injections of oHSV between 2 and 6 weeks postinduction of CHST.

Results: The *P. aeruginosa* inoculation plus double EAC ligation technique successfully induced a range of CHST growth in 100% of the ears in the model-development group. Osteolytic effects of CHST were observed in 6% of ears whereas osteoblastic effects were observed in 31% of ears. CHST volume decreased by 50% or more in 12 of the 20 ears in the oHSV-treatment groups. An apparent reversal of osteoblastic effects was also observed in three out of four ears 6 weeks following the third oHSV injection.

Conclusions: *P. aeruginosa* inoculation plus double EAC ligation reliably induces CHST formation in gerbil. CT-based volumetric measures are significantly more accurate than single-slice morphometric area measures for quantification of CHST size. Treatment with oHSV appears to be efficacious for reducing CHST volume by as much as 77% with as few as one treatment.

Key Words: Cholesteatoma, oncolytic virotherapy, oHSV.

Level of Evidence: NA

INTRODUCTION

Although Duverney first described cholesteatoma (CHST) of the temporal bone in 1683, it was not until

This is an open access article under the terms of the Creative Commons Attribution-NonCommercial-NoDerivs License, which permits use and distribution in any medium, provided the original work is properly cited, the use is non-commercial and no modifications or adaptations are made.

From the Department of Otolaryngology–Head and Neck Surgery (R.N.S., B.R.E., N.L.), University of Cincinnati College of Medicine, Cincinnati, Ohio, U.S.A.; Neurosensory Disorders Center at University of Cincinnati Gardner Neuroscience Institute (R.N.S.), Cincinnati, Ohio, U.S.A.; Cincinnati Children's Hospital Medical Center (R.N.S.), Cincinnati, Ohio, U.S.A.; Department of Communication Sciences and Disorders (B.R.E., I.S.), University of Cincinnati College of Allied Health Sciences, Cincinnati, Ohio, U.S.A.; Center for Childhood Cancer and Blood Diseases (M.C., T.C.), The Research Institute at Nationwide Children's Hospital, Columbus, Ohio, U.S.A.; Division of Hematology, Oncology, Blood and Marrow Transplant, Department of Pediatrics (T.C.), Nationwide Children's Hospital, Columbus, Ohio, U.S.A.

Funding and Conflict of Interests: Funding for this work was provided by University of Cincinnati's College of Medicine, Center for Clinical and Translational Science and Training, and Bearcats Against Cancer Fund of the Department of Radiation Oncology. Dr. Ravi N. Samy has received research support and consulting honoraria from Cochlear Corporation.

This work was accepted as a Triological Society thesis (Thesis # 2019-22) and won the Honorable Mention award in the Basic Science category. It will be presented at the Triological Society Combined Sections Meeting in January 2020.

Send correspondence to Ravi N. Samy, MD, FACS, Department of Otolaryngology–Head and Neck Surgery, University of Cincinnati College of Medicine, Cincinnati Children's Hospital Medical Center and Neurosensory Disorders Center at University of Cincinnati Gardner Neuroscience Institute, 213 Albert Sabin Way, MSB 6407, Cincinnati, OH 45267-0528. E-mail: ravi.samy@uc.edu

DOI: 10.1002/liv.2.307

1838 that Johannes Mueller first coined the term.¹ CHSTs have been known to be proliferative, erosive, and destructive lesions that are usually acquired but can also be congenital in origin. CHSTs cause significant morbidity and mortality worldwide as they can affect both pediatric and adult populations. While some CHSTs may be asymptomatic, they typically cause symptoms ranging from mild hearing loss and otorrhea to complete deafness, dizziness, facial nerve paralysis, brain abscess, meningitis, and even death.² The annual incidence is approximately 3–6/100,000 in children and 9/100,000 in adults, with a slight male predominance.³ Based on the above epidemiologic data, in the United States alone, there may be 15,000 new cases per year, which does not include recidivistic disease.

The only available definitive therapy for CHSTs is surgery to eradicate the lesions and prevent progression. However, there is a recurrence rate ranging from 15% to 60%, depending on the age range and population studied, duration of follow-up, and type of surgery performed.⁴ The high rate of recurrence is due to the difficulty of surgically removing all microscopic disease (creating residual disease) or due to recurrence of a retraction pocket and squamous debris accumulation resulting in regrowth of CHSTs. In addition to surgery, otolaryngologists also use medical management, which may reduce the growth rate of CHSTs. Nonsurgical management consists of dry ear precautions and ototopical antibiotics to stop the purulent discharge due to associated biofilm formation and infection.^{5,6} While medical management minimizes some of

the symptoms associated with CHSTs, it does not eradicate the lesions or completely prevent future growth. In addition, given the high cost of surgical interventions and high rate of recidivism, CHST in developing countries can often be inadequately addressed. Therefore, there is an important need for new and affordable approaches in the treatment and management of CHSTs.

Oncolytic virotherapy (OV) is emerging as a promising therapeutic approach for the treatment of human and animal malignancies.⁷ Oncolytic viruses selectively infect, replicate in, and kill the target cells while sparing normal tissues.⁸ They exert their effect by direct lytic effect as well as by immunomodulation.⁹ Cell selectivity has been achieved by using viruses that are not virulent in humans or via genetic engineering.⁸ Although OV was first described a century ago in the French literature, it has not been until the past decade that the technique has grown in significant utilization, success, and understanding.^{10–12} In fact, in 2015, the U.S. Food and Drug Administration (FDA) approved the first OV for the treatment of metastatic melanoma (talimogene laherparepvec [T-VEC]).¹³ Oncolytic herpes simplex virus (oHSV) is the most commonly used vector for OV; it has been used in clinical trials for pulmonary cancer, prostate cancer, malignant melanoma, and sarcomas. In addition, it has been used for both intracranial and nervous system tumors such as gliomas, glioblastomas, and malignant peripheral nerve sheath tumors. This virus has been shown to be both safe and effective in both animal models (eg, nude mouse and monkey) as well as in pediatric and adult human populations.^{14–24}

While CHST is not a true neoplasm, we hypothesized that oHSV can selectively eradicate CHST in vivo in a gerbil model based on the previous experiments in our lab indicating selective lethality of oHSV against CHST cells in vitro.²⁵ The rationale for using oHSV to treat CHST was based on the fact that wild-type herpes simplex virus (HSV) is a lytic virus that can infect a wide range of cells including epithelial cells (eg, herpetic gingivostomatitis and herpetic whitlow). Furthermore, CHST matrix is composed of epithelial cells. oHSV is attenuated and can be mutated to grow preferentially in dividing cells (as is found in CHST).^{14,22} Additionally, CHST is associated with bacterial superinfection and biofilm formation, which can prime the body for an immune response that is low grade and potentially chronic in nature.^{5,6} We postulate that acute oHSV infection might facilitate this immune response and lead to eradication of CHST.

In this study, we first assessed the effectiveness of our in vivo technique to induce CHST formation by inoculation of each external auditory canal (EAC) with *Pseudomonas aeruginosa* with ligation of the canals. We compared morphometric and volumetric analyses using high-resolution micro-computed tomography (micro-CT) to determine the most accurate method to quantify CHST size and any associated osteolytic or osteoblastic changes. Then, treatment efficacy with one to three intrabullar injections of oHSV was compared in an additional group of gerbils with induced CHST. The potential relevance of these findings may alter the clinical landscape for future CHST management as a novel and minimally invasive,

postsurgical adjuvant therapy that may reduce risk of lesion progression or recurrence.

METHODS

This study was performed in accordance with the Public Health Service (PHS) Policy on Humane Care and Use of Laboratory Animals, the National Institutes of Health (NIH) Guide for the Care and Use of Laboratory Animals, and the Animal Welfare Act (7 U.S.C. et seq.). The animal use protocol was approved by the Institutional Animal Care and Use Committee (IACUC) at our institution.

An in vivo CHST model was developed using a double EAC ligation approach in a group of 16 Mongolian gerbils (Charles River Laboratories). The general approach of using EAC ligation has been shown to create gerbilline CHSTs that are histologically identical to the spontaneous gerbilline CHSTs. The induced CHSTs simulate the human condition as they can erode the labyrinth and enter the intracranial cavity.^{26,27} The gerbil CHST model was then utilized for preliminary testing of the treatment efficacy of oHSV in an additional group of 10 gerbils.

Female Mongolian gerbils, weighing between 50 and 70 g, were anesthetized with sodium pentobarbital in preparation for the ligation procedure. An initial dose of 70 mg/kg was followed by subsequent maintenance doses of 1/3 relative to the initial dose in 45-minute intervals. The double-ligation approach was completed bilaterally to induce CHST growth. Postauricular incisions were made to access the cartilaginous portion of the EAC. The EAC was transected 2–3 mm laterally from the osseocartilaginous junction, and 20 μ L of *P. aeruginosa* (1×10^4 colony forming units [CFU/mL]) was injected into the bony EAC lumen. Inoculation of the EAC with *P. aeruginosa* plus EAC ligation has been demonstrated to induce CHST formation in 2–6 weeks as opposed to 6 months for CHST formation with EAC ligation alone.²⁸ Braided silk sutures were used bilaterally for the medial and lateral EAC ligations in horizontal mattress fashion, and the skin incision was closed with interrupted absorbable sutures (see Fig. 1A).

The inoculation solution was prepared with a strain of *P. aeruginosa* obtained from the American Type Culture Collection (ATCC; PA01-AC, No. 47085). The *P. aeruginosa* was plated on 100 mm sterile Luria broth agar plates (1.0% tryptone, 0.5% yeast extract, 1.0% sodium chloride, and 1.5% agar) and cultured at 37°C for 24–48 hours prior to being used for EAC inoculation. The solution used for EAC inoculation was made by transferring small samples of *P. aeruginosa* from the culture plate into a vial of RapID inoculation fluid (ThermoFisher Scientific). The specified dilution of 1×10^4 CFU/mL was confirmed by measuring the turbidity of the solution using a BioMate3 spectrophotometer (ThermoFisher Scientific).

The oHSV for this study was propagated in baby hamster kidney cells and then purified using standard virology techniques. Following purification, oHSV was suspended in cell media (Dulbecco's modified eagle's medium, Millipore-Sigma) and 10% glycerol (50 μ L total

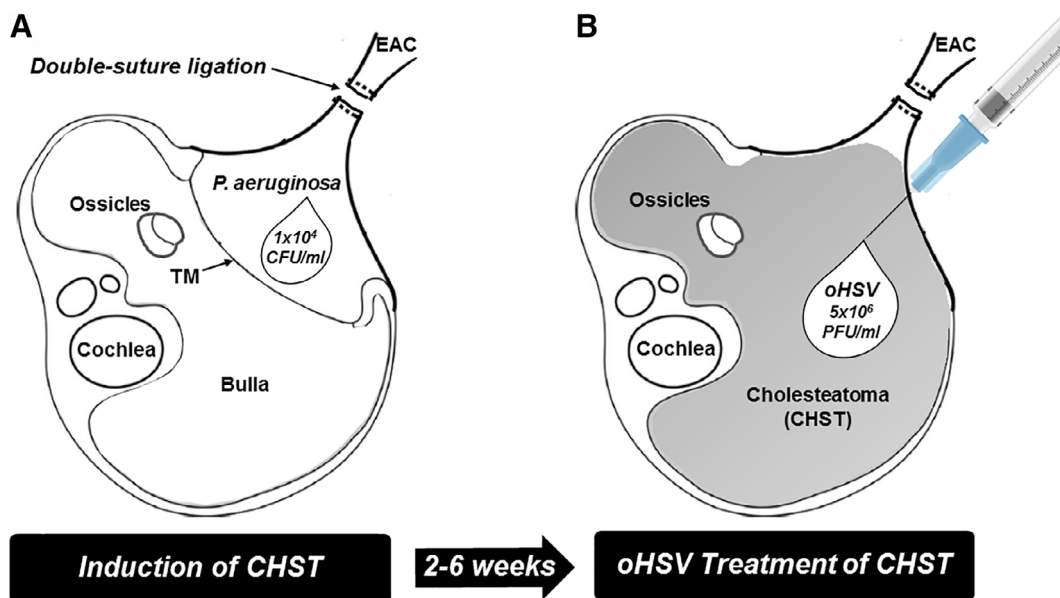


Fig. 1. The *P. aeruginosa* inoculation plus double EAC ligation approach (A) was used to induce CHST. (B) The intrabullar route and concentration of the oHSV injections that were tested as a CHST treatment. Anatomy schematics adapted with permission from Yamamoto-Fukuda et al, *Am J Pathol*, 2010, 176 (6), 2602–2606.²⁹ CHST = cholesteatoma; EAC = external auditory canal; oHSV = oncolytic herpes simplex virus; TM = tympanic membrane.

volume) and stored at -80°C until injection. The oHSV was prepared for injection by diluting it in sterile phosphate-buffered solution to a concentration of 5×10^6 plaque forming units per milliliter (pfu/mL). A total of $100 \mu\text{L}$ of this dilution were taken up into a 1 mL syringe with a 27G needle for injection through the bony EAC and into the bullar space (see Fig. 1B).

Six weeks following inoculation and ligation, the 16 gerbils in the model-development group were euthanized and perfused with paraformaldehyde before undergoing micro-CT imaging. The 10 gerbils in the oHSV treatment groups were sedated with isoflurane and underwent in vivo micro-CT imaging at multiple time-points. At 2 weeks post-CHST induction, all 10 animals underwent pretreatment micro-CT imaging followed by the initial bilateral oHSV injections. The five animals in the one-treatment group (oHSVx1) underwent post-treatment micro-CT imaging at either 3 weeks or 4 weeks following the single oHSV injection. The three animals in the two-treatment group (oHSVx2) and the two animals in the three-treatment (oHSVx3) groups received follow-up micro-CT imaging and oHSV injections in 1-week intervals. The final post-treatment micro-CT scans were completed 3 weeks following the last injection of the respective groups (Fig. 9A).

The micro-CT imaging was completed with a Siemens cone-beam micro-CT unit (Tarrytown, NY) with a protocol that lasted 18 minutes and used the following parameters: 80 kilovoltage peak (kVp) tube potential, 500 microamperes (μA) tube current, and 1,050 ms integration time per stop. The images were reconstructed with $36\text{-}\mu\text{m}$ isovoxel resolution. Morphometric and volumetric analyses using Siemens Inveon Research Workplace software were then performed to determine the size of CHST and any associated osteolytic or osteoblastic changes. Reconstructed CT images were saved as tagged

image file format (tiff) files for two-dimensional (2D) morphometric analysis of CHST size and the extent of bony changes using ImageJ software (NIH public domain). One representative micro-CT slice in the axial plane was chosen for morphometric analysis based on the following criteria: 1) Bony shell of the middle portion of the cochleae and/or bony ring around the modiolus within view and 2) Superior portion of the malleus within view. Quantitative analyses of CHST size were subsequently completed on a sample of 10 from the group of 16 gerbils. Morphometric size of CHST was determined by calculating the surface area in mm^2 of the gray voxels within the bullar space (which contrasts with the white pixels representing bone and the black pixels representing air-filled spaces). Surface area of the total bullar space (minus the bony area of the malleus) was measured in mm^2 , which allowed the calculation of CHST size as a percentage of the total bullar space. Width of the bony rim of the EAC was measured to estimate osteolytic changes related to the canal portion of CHST.

Three-dimensional (3D) volumetric analyses of CHST size were also completed in a subset of animals from the model-development group to visualize the extent of CHST growth throughout the bullae. Volumetric measures are hypothesized to more accurately estimate the total CHST volume compared with the 2D surface area measurements described above. The measures of CHST volume were completed by digitally labeling the gray voxels indicating presence of CHST across all CT slices using the voxel-labeling tool within Siemens Inveon postprocessing software. The volume of the CHST in mm^3 is then derived by the software using a 3D compilation of the CHST masses within the gerbil bullae. CHST stage was also classified according to a modification of the Chole et al classification system (Table I).^{26,27}

TABLE I.
Stages of Gerbilline Cholesteatoma Adapted From the
Classification System of Chole and Colleagues.^{23,26}

Stage	Findings
I	Accumulation of keratin without displacement of the tympanic membrane
II	Medial displacement of tympanic membrane without contact with the cochlea
III	Medial displacement of tympanic membrane with contact with the cochlea
IV	Involvement of the entire bulla with or without cochlear fistula
V	Involvement of the entire bulla and intrusion into cranial fossa

Following completion of micro-CT imaging, the gerbils' skulls were inspected and dissected under a surgical microscope. During dissection, indicators of EAC and middle ear pathology and the presence of CHST were noted (eg, keratin debris, granulation tissue, presence of purulent effusion, ossicular erosion, cranial erosion, thickness of bony wall of bulla). Photographs of the bulla were captured at $\times 4$ magnification using the iMicroscope application for iPhone (version 2.0, elklab UG).

Statistical analysis

Correlation and linear regression analyses and a Bland Altman analysis²⁷ were completed to assess the differences between the two quantitative measures of CHST size: 1) morphometric measures of CHST area in one representative micro-CT slice in the axial plane, and 2) volumetric measures of CHST volume in all micro-CT slices in the axial plane containing the bulla (generally 250–300 slices). The correlation and linear regression analyses were completed to assess the general relationship between the two measurement techniques. The Bland Altman analysis technique was utilized to quantify the mean difference and range of differences between the two quantitative measures.³⁰ This analysis technique is commonly used to compare quantitative measures obtained with a new technique to those obtained with an established

measure. The Bland Altman plot also includes 95% confidence intervals around both the mean difference between the measures and around the upper and lower limits of agreement of the sample data. The key interpretation of the Bland Altman plot relates to the relationship between the 95% percent confidence interval around the mean of the difference between the measures and the line of equality (ie, zero line). Specifically, if the confidence interval around the mean difference does not include zero, the new technique is considered to be significantly biased/different compared to the established technique.

Paired-sample *t* tests were used to assess the within-group treatment effects of oHSV against CHST volume in the 10 animals that received either one, two, or three injections of oHSV. Treatment response rate was also assessed according to previous research in the oncology literature that designates a given lesion as stable if there is less than a 50% reduction in size post-treatment.³¹ The designator of partial response is given to those lesions that decrease in size by more than 50% but less than 100%, which would denote a complete response.

RESULTS

The double EAC ligation technique plus *P. aeruginosa* inoculation reliably led to CHST growth in ears within the 2–6 week time frame for gerbils in both groups. In the initial group (n = 16 gerbils, 32 ears), CHST growth was observed in 100% of ears and ranged from stage II to V^{26,27} with 63% of the gerbils exhibiting different stages across ears. Osteoblastic effects were observed in 31% of ears while only 6% of ears exhibited osteolytic effects as a result of CHST presence (see representative images in Fig. 2).

During the period following *P. aeruginosa* inoculation and EAC ligation, 50% of gerbils scratched off a portion or all of their pinnae. This observation is shown in Figure 3B and was thought to be a sign of pruritus at the site of the skin incision or a response to an infectious process triggered by the *P. aeruginosa*. However, the lateral sutures remained intact for 68% of the 32 gerbil ears while the medial sutures remained intact for 72% of ears.

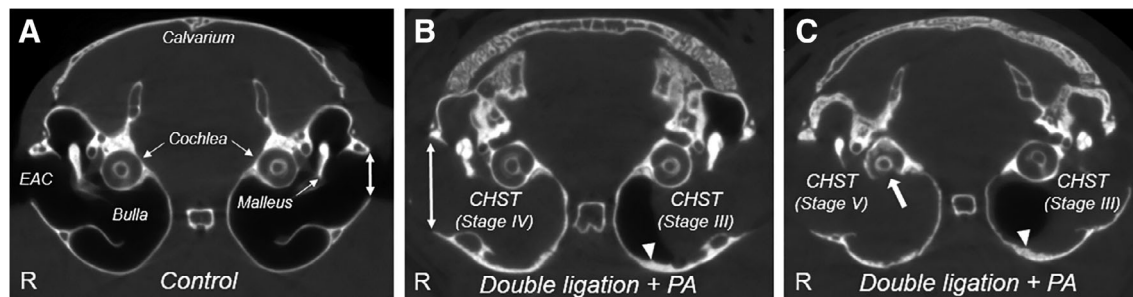


Fig. 2. Gray voxels in axial micro-computed tomography slices indicate CHST in both the right and left bullae of two representative animals in panels (B) and (C) that are in contrast with the normal control animal in panel (A). Panel (B) shows stage IV CHST filling the right bulla and stage III CHST partially filling the left bulla 6 weeks post *P. aeruginosa* inoculation and EAC ligation. Bony EAC erosion is indicated by the vertical double-arrow in panel (B) (EAC width is nearly double the width of the left EAC of the control animal in panel A). (C) Stage V CHST in the right bulla includes erosion of the bony wall of the cochlea (arrow) and minor intracranial intrusion (revealed in additional slices not shown above). Arrowhead symbols in panels (B) and (C) indicate regions of osteoblastic effects, which are in stark contrast to the thin bulla wall of the control gerbil. CHST = cholesteatoma; EAC = external auditory canal; PA = *Pseudomonas aeruginosa*.

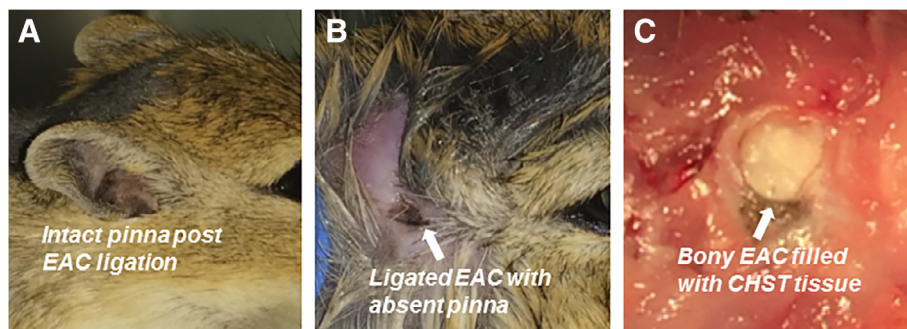


Fig. 3. Representations of normal pinna anatomy preserved after EAC ligation (A) compared to absent pinna (due to animal scratching) post-ligation (B). Representative appearance of CHST mass filling bony portion of EAC 6 weeks following *P. aeruginosa* inoculation and EAC ligation (C). CHST = cholesteatoma; EAC = external auditory canal.

TABLE II.

Dissection Observations for Animals in the Model-Development Group (n = 16 animals, 32 ears) Are Listed According to the Classification System of Chole et al.^{23,26}

CHST Stage*	Number of Ears	Common Dissection Observations	Pinna Intact	Medial Ligation Intact	Lateral Ligation Intact
II	3/32	K, BT, BF	0/3	2/3	1/3
III	22/32	K, GT, BT, OE	9/22	14/22	14/22
IV	6/32	K, GT, BT, PEB	6/6	6/6	6/6
V	1/32	K, GT, PEB, CE	1/1	1/1	1/1

*CHST stage was determined via assessment of micro-CT slices.

BF = biofilm; BT = bullar thickening; CE = cranial erosion; CHST = cholesteatoma; GT = granulation tissue; K = keratin debris; micro-CT = micro-computed tomography; OE = ossicular erosion; PEB = purulent effusion in bulla.

Table II provides a count of the number of ears observed within each stage for the animals in the initial CHST development group. Stage III CHST (ie, displacement of the medial portion of the tympanic membrane [TM] with CHST contact with the cochlea without involvement of the entire bulla) was the most commonly observed stage among the initial group. Stage IV CHST (ie, involvement of the entire bulla) was the second most common stage observed for the initial group. Two-dimensional analysis in ImageJ revealed thickening of the bulla in 25 of 32 ears while minimal osteolytic effects were observed. The arrowheads in Figure 2B, 2C point out regions of bullar thickening following CHST induction. The long arrow in Figure 2C indicates a

region of erosion of the cochlear bony wall with CHST involving the entire bulla.

Of the 16 gerbils that underwent *P. aeruginosa* inoculation and EAC ligation, a subset of 10 were chosen for comprehensive morphometric and volumetric analysis using the Siemens Inveon Research Workplace software. Figure 4A, 4B represents the morphometric and volumetric micro-CT analyses, respectively. Figure 4B illustrates the 3D compilation of the micro-CT scans overlaid with the software-generated CHST masses based on the digital labeling in red for the CHST in the right bulla and in blue for the CHST in the left bulla.

Figure 5A, 5B shows the summary of the morphometric and volumetric analyses for the sample of 10 gerbils.

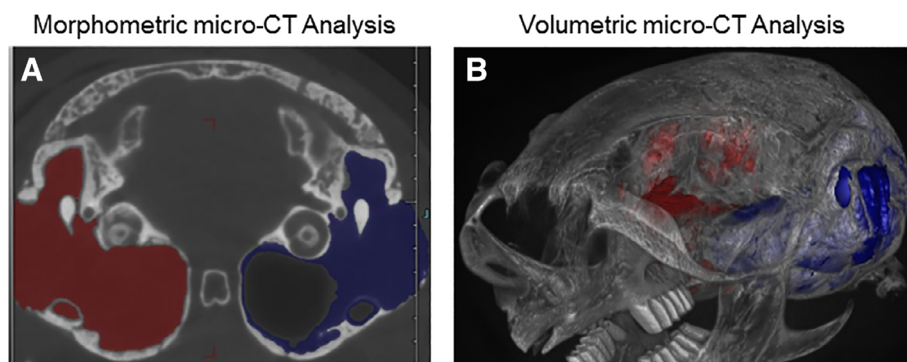


Fig. 4. Representations of morphometric (A) and volumetric (B) analysis techniques for quantification of CHST surface area and volume, respectively. Colored areas (red = right ear; blue = left ear) represent digital labeling of CHST in one micro-CT slice in the axial plane (A) and across all micro-CT slices containing the CHST in the 3D compilation (B). CHST = cholesteatoma; micro-CT = micro-computed tomography.

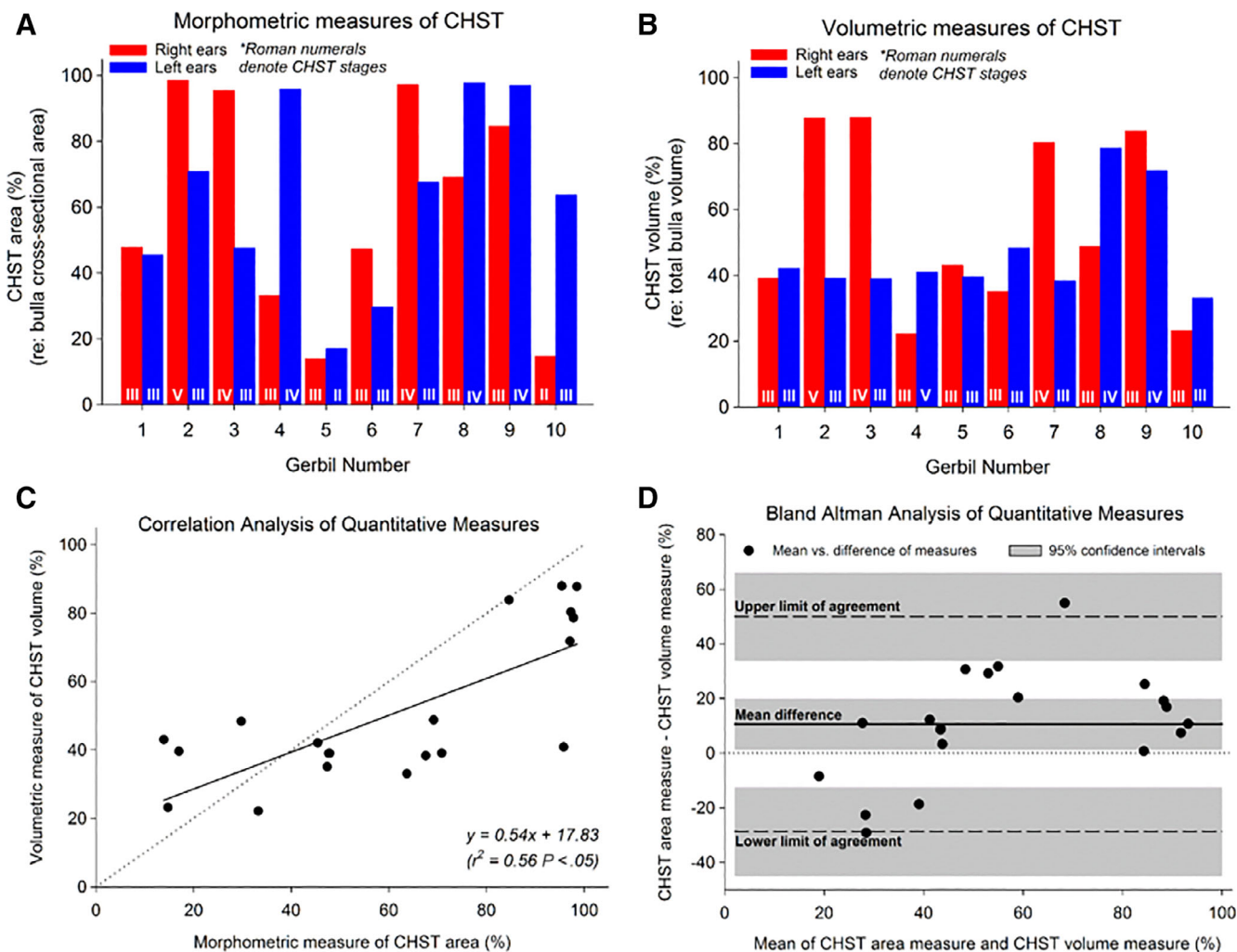


Fig. 5. Within-group comparisons of CHST quantification indicated that morphometric calculations of CHST area (A) generally overestimate CHST volume (B). The stages of CHST formation for each ear are noted in Roman numerals at the bottom of panels (A) and (B). Correlation analysis in panel (C) revealed a significant positive correlation between the two measures, although significant scatter around the regression line is noted as well as the departure from unity (dotted line). The Bland Altman plot in panel (D) indicates that the difference between the two measures is just over 10% on average (mean difference line), but could also be overestimated by 66% (upper boundary of upper limit of agreement) or underestimated by -45% (lower boundary of lower limit of agreement). CHST = cholesteatoma.

from the initial group. The morphometric measures (Fig. 5A) generally overestimated CHST size in the majority of gerbils when compared to the more comprehensive volumetric measures (Fig. 5B). The maximum overestimation is near a factor of 2 (eg, Gerbil 4, left ear) while the maximum underestimation shows the morphometric estimate to be less than half the volumetric measure (eg, Gerbil 5, right ear).

Linear correlation analysis of the two quantitative measures (Fig. 5C) indicated that the morphometric measures of CHST area are significantly correlated with the volumetric measures of CHST volume ($r^2 = 0.56$, $P < .05$). However, the y-intercept of the equation that describes the relationship ($y = 0.54x + 17.83$) suggests that the measures differ by at least 17.83%. In addition, the r^2 value of 0.56 indicates that the morphometric measure of CHST area only explains 56% of the variance in the volumetric measures.

To characterize the mean difference and the range of agreement between the two quantitative measures, a

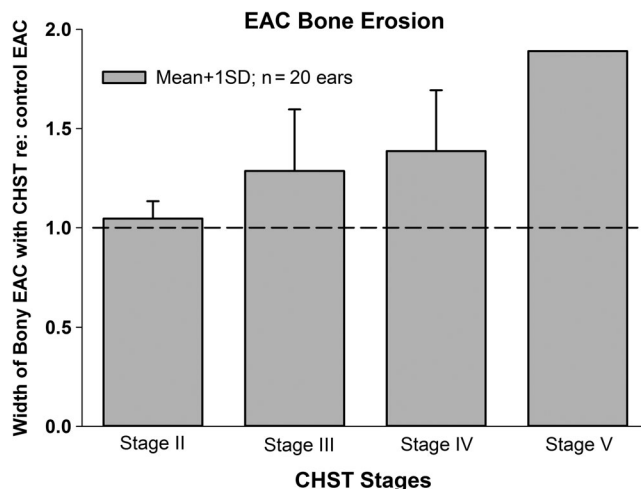


Fig. 6. Width of bony EAC (re: normal EAC control) increases from CHST stage II to stage V. CHST = cholesteatoma; EAC = external auditory canal.

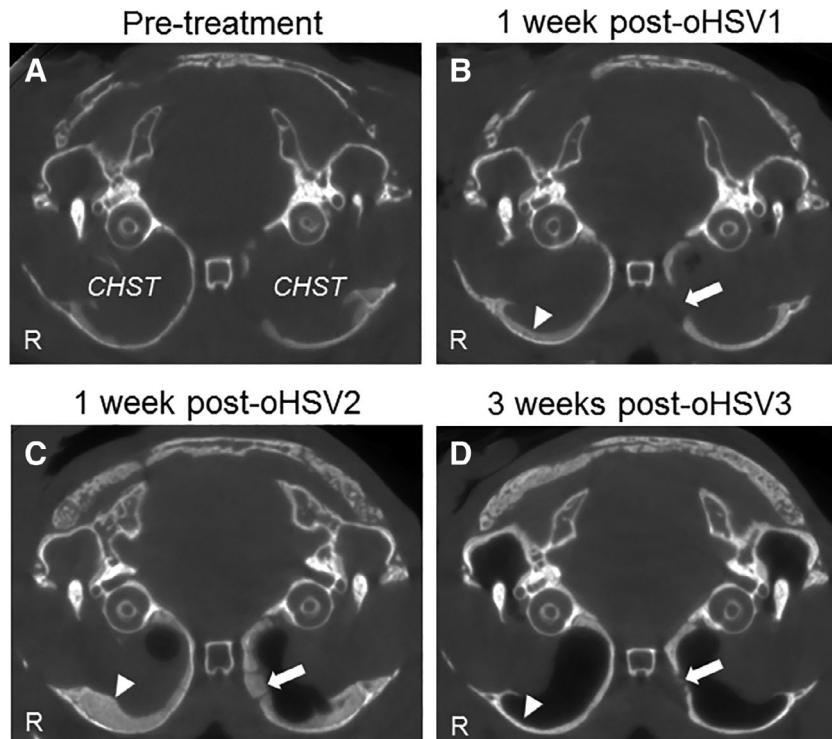


Fig. 7. Serial micro-computed tomography scans in the axial plane of one animal at the following time points: (A) Pretreatment (2 weeks postinduction of CHST); (B) 1 week post first dose of oHSV; (C) 1 week post second dose of oHSV; and (D) 3 weeks post third dose of oHSV. The CHST masses (denoted by areas of gray voxels within the bullae) are considerably reduced in area in panel (D) compared to previous time points (A–C). Also of note, is the region of osteolytic changes in panel (B) and (D) (arrow symbols) and regions of osteoblastic responses in panel (B) and (C) (white arrowhead symbols). CHST = cholesteatoma; oHSV = oncolytic herpes simplex virus.

Bland Altman plot was constructed (Fig. 5D). The mean difference according to this analysis was 10.63% (indicated by solid horizontal line in Fig. 5D) and the 95% confidence interval around that mean difference (gray area) does not include the line of equality (zero line indicated with dotted line in Fig. 5D). This finding indicates that the CHST area measure is significantly biased/different from the volumetric measures. The upper and lower limits of agreement (dashed lines) along with their respective confidence intervals indicate that the magnitude of the error of the morphometric

CHST area measure could be as high as 66% (ie, overestimation) and as low as -45% (ie, underestimation).

Figure 6 shows the calculations of width of the bony EAC in animals in the initial group with CHST as a ratio relative to the width of the bony EAC of normal control animals. This metric has been used by Chole and colleagues to gauge the osteolytic effects of CHST.¹⁴ The trend in the plot suggests that the magnitude of osteolytic changes within the EAC increases as the CHST increases from stage II to stage V.

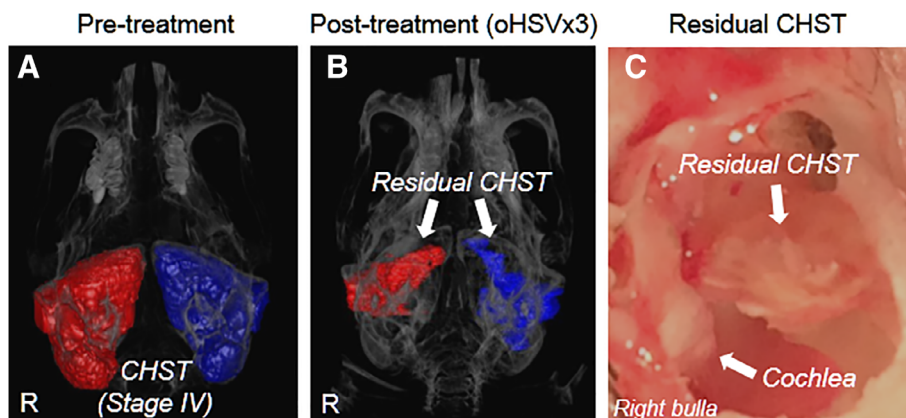


Fig. 8. (A, B) Volumetric reconstruction of CHST in the same animal whose morphometric images are shown in Figure 7. The micrograph in panel (C) illustrates the residual CHST in the right bulla at 3 weeks following the third oHSV treatment as well as a near-normal pinkish-white appearance of the bulla cavity and the bony cochlear wall. CHST = cholesteatoma; oHSV = oncolytic herpes simplex virus.

oHSV Treatment Groups

The micro-CT scans at four different time-points for one representative animal in the oHSV treatment group that received three oHSV injections are presented in Figure 7. The pretreatment scan (ie, 2 weeks following *P. aeruginosa* inoculation and EAC ligation) shows stage IV CHST occupying the entirety of both bullae (Fig. 7A). The following micro-CT scan at 1-week following the first injection of oHSV (oHSV1; Fig. 7B) indicates minimal effect of the treatment in the left bulla. The image in Figure 7C was acquired 1 week following the second oHSV treatment (oHSV2) and shows the emergence of air pockets within the bullae, which corresponds to a decrease in CHST volume. After a third oHSV treatment (oHSV3; Fig. 7D), the volume of the CHST in both bullae decreases further. The

regions of osteolytic changes and the regions of osteoblastic response are improved after oHSV treatment.

Figure 8A, 8B shows the 3D compilations of the micro-CT scans overlaid with the volumetric measures of the CHST for the same animal whose images are shown in Figure 7. The volume of the CHST decreased by 72% following three treatments with oHSV (panel B) relative to the pretreatment CHST volume (panel A). In addition to this substantial reduction in CHST volume, the thickness of the bulla at 3 weeks post-oHSV3 (Fig. 7D) is nearer that of the pretreatment scan (Fig. 7A). Post-imaging and postethanasia dissection of the bulla (Fig. 8C) revealed a small residual CHST mass with the cochlear and bullar bone similar in appearance (ie, pinkish-white) to those of control animals.

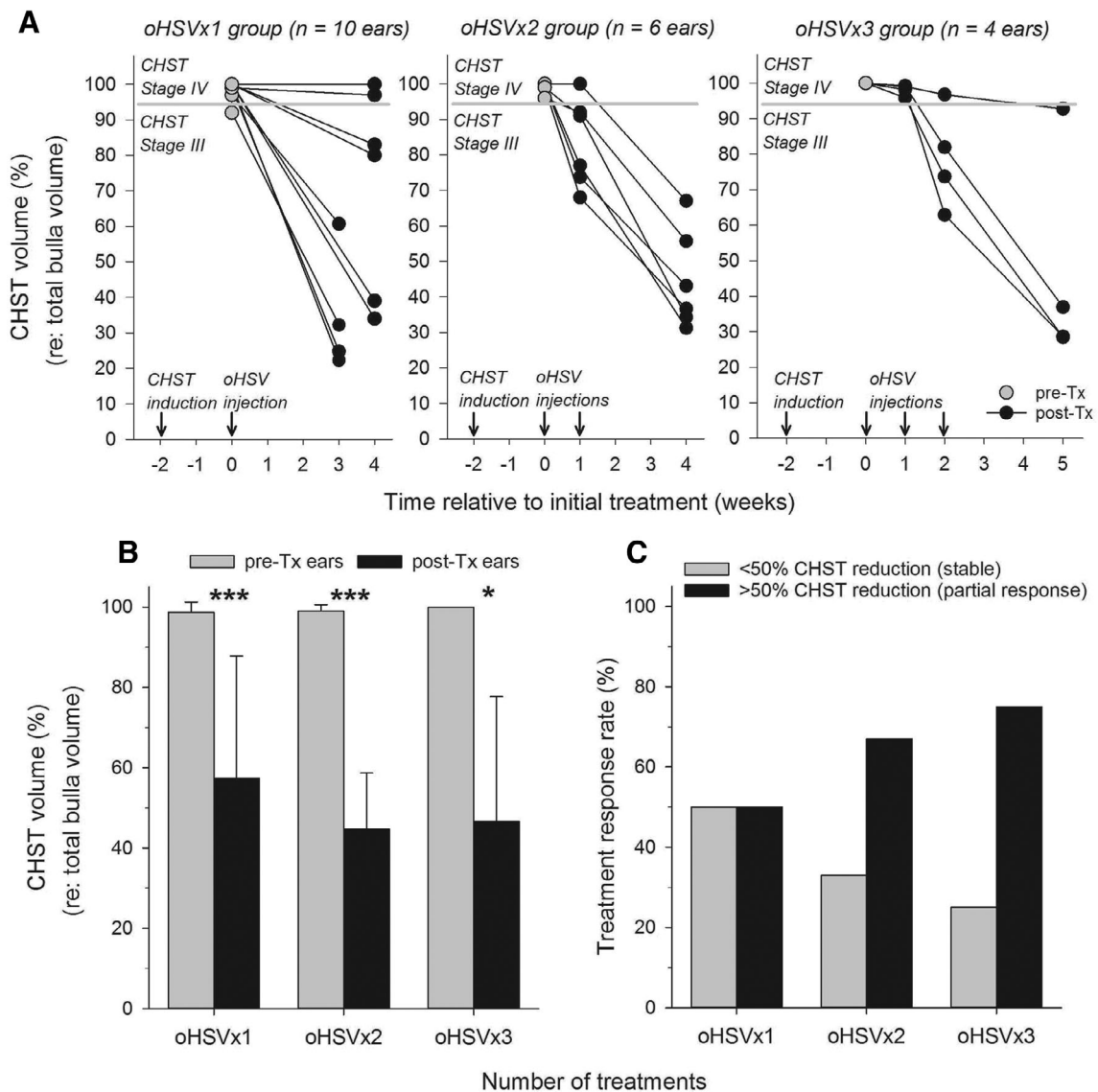


Fig. 9. Preliminary evidence suggesting treatment efficacy of oHSV against CHST. CHST volume decreased by as much as 70% and the majority of ears changed from stage IV to stage III following one, two, or three oHSV treatments (plots in panel A). Within-group statistical analyses of pretreatment (pre-Tx) versus post-treatment (post-Tx) effects revealed statistically significant reductions in CHST volume for all three treatment groups (panel B; * $P < .05$; *** $P < .001$). Panel (C) indicates improvement in treatment response rate as the number of treatments increases. CHST = cholesteatoma; oHSV = oncolytic herpes simplex virus; Tx = treatment.

Preliminary evidence for the efficacy of oHSV against CHST is illustrated across the oHSVx1, oHSVx2, and the oHSVx3 treatment groups in Figure 9A. Overall, treatment with oHSV reduced CHST volume (measured with the volumetric technique) by 20% or more in 85% (17/20) of the ears treated. This reduction of CHST volume is also indicated by the large majority of the ears changing from a classification of stage IV pretreatment to stage III post-treatment (see Table I). CHST volume reductions as great as 70% were observed among a portion of the ears receiving one, two, or three injections of oHSV. In three of the four ears (75%) of the gerbils receiving three oHSV treatments, an apparent reversal of osteoblastic effects was also observed.

The results of the paired-sample *t* tests indicate significant reductions in CHST volume for the oHSVx1, oHSVx2, and oHSVx3 treatment groups. The calculations of treatment response rate in Figure 9C are based on the count of ears above (ie, stable) versus below (ie, partial response) the gray line of 50% across the three plots in Figure 9A. This criterion of treatment effect is used in the oncology literature to discuss immunotherapy because it has shown to be clinically meaningful in that those individuals who achieve a 50% tumor reduction (partial response) have a high probability of survival.³¹ The trend observed in Figure 9C suggests an increase in ears with >50% reduction in CHST volume as the number of treatments increases.

DISCUSSION

In this pilot study using a gerbil model of CHST, our technique of *P. aeruginosa* inoculation plus double-EAC-ligation reliably induced and expedited CHST formation. CHST size and associated bony changes were reproducibly measured and quantified using morphometric and volumetric techniques as noted by high-resolution micro-CT. Following oHSV treatment, a decrease in CHST volume was seen as was reversal of osteoblastic effects. Our novel application of oHSV to treat CHST yielded encouraging preliminary findings, suggesting its possibility as a future alternative to traditional surgical therapies.

OV is emerging as a promising new therapeutic approach for human cancer treatment.¹⁴ Numerous viruses have been utilized, including reovirus, adenovirus, vaccinia virus, and oHSV. oHSV was the first genetically engineered virus to be used for OV, as reported in 1991; this particular mutant virus is a thymidine-kinase negative variant that was initially utilized in human glioma cell lines (including an astrocytoma and a glioblastoma) as well as in a nude mouse model.³² This virus showed the ability to replicate in actively dividing cell lines (ie, tumor) while being impaired to replicate in nondividing cells or in a control mammalian nervous system.^{14,22} In the nude mouse model of glioma, oHSV treated tumors were significantly smaller than control tumors by day 26 after injection. Thus, arming an oncolytic virus with therapeutic genes has demonstrated enhanced antitumor effects.³³ Since the initial oHSV experiments in 1991, attenuated oHSV mutants engineered with deletions of normally critical genetic functions that are dispensable in cancer cells

are being actively pursued as novel therapeutic agents by many investigators and pharmaceutical companies.²⁴ The goal is to enhance OV efficacy by arming the chosen virus with therapeutic transgenes suited for the particular tumor being treated.³⁴

There are numerous encouraging reports of early phase clinical trials exploring the safety of administering variety of attenuated oHSV mutants to humans by intracranial, intralesional, and hepatic artery routes.^{17,35,36} Systemic routes of OV administration are felt to be of importance in metastatic disease.³² All of the OV studies completed thus far have confirmed safety at the doses tested with no serious adverse events reported. In 2013, Amgen reported initial positive results of the first phase III trial of T-VEC, an oHSV expressing granulocyte-macrophage colony-stimulating factor used for the treatment of metastatic melanoma.³⁷ Based on the initial safety and subsequent efficacy (with regression in injected lesion size and distant metastases), the FDA approved the drug for clinical use.³⁸

The application of oHSV to treat a benign disease such as CHST is novel. According to a search of the current literature, we are the first to use OV for eliminating benign CHST cells as an alternative or adjuvant to a traditional therapy (ie, surgery).²⁵ Because CHST is not a true neoplasm, unlike the other tumors for which OV has been used, only local (and not systemic) therapy is all that is indicated. Thus, this treatment may be best for microscopic disease after surgical treatment or when the disease burden of CHST is limited (eg, pars flaccida retraction pocket with early CHST formation). As opposed to concern about resistance to therapy in the treatment of malignancies, patients with CHST can continue to have multiple surgeries for recurrent disease. However, there is the risk of significant iatrogenic injury, particularly in inexperienced hands. Additional studies of oHSV and other types of OV for CHST may show that combining OV with medical therapy (eg, otological and/or systemic antibiotics and steroids) may reveal synergistic and additive effects, as has been demonstrated with OV in other tumors.

CHST can be dangerous due to complex and multifactorial mechanisms. They have the ability to cause bone erosion due to concomitant granulation tissue and involved inflammatory response involving mediators and cells such as macrophages, monocytes, osteoclasts, and mast cells. At the cellular level (ie, the level of the tumor microenvironment), cytokines and nitric oxide are involved.^{39,40} These cytokines include epidermal growth factor, tumor necrosis factor, and interleukins and work in conjunction with nitric oxide to activate osteoclasts and result in bone destruction, which can eventually lead to deafness, dizziness, facial palsy, and/or intracranial involvement. In addition, lipopolysaccharides, which are found in bacterial cell walls, have been found in higher concentrations in CHSTs with bone erosion as compared to CHSTs without associated bone erosion.⁴¹ While CHST surgery has advanced and evolved over the past 100 years, including the use of laser or endoscopic techniques in addition to standard microscopic techniques (eg, canal wall up or down mastoidectomy with or without mastoid obliteration), recidivism is a

significant concern.^{29,42–45} Creating a minimally invasive and relatively affordable option may simplify and provide substantial advantages in combination with the current surgical treatment by providing a targeted and novel treatment strategy.¹⁵

CHST occurs primarily due to a lack of growth control involving the skin of the EAC and the epidermal layer of the TM.²⁹ Gerbils are an ideal model for translational research on CHST as they are the only nonprimate animals that have been shown to spontaneously grow CHST.²⁷ Similar to humans, the gerbil CHST is caused by an accumulation of keratin on the TM that advances medially, leading to bone resorption. While staging of gerbil CHST was performed in the past by opening the bulla, micro-CT has been shown more recently to noninvasively identify the extent of CHST in the bulla.²⁸ Although gerbils can spontaneously form CHST, EAC ligation has been shown to expedite growth, usually within 3–6 months.²⁷ Furthermore, the addition of *P. aeruginosa* can more rapidly create CHST that are typically larger and more destructive, usually within 6 weeks.²⁸ Overall, the double-ligation plus *P. aeruginosa* inoculation technique was highly successful in inducing CHST in gerbils. Given that a slightly larger percentage of lateral ligations remained intact compared with medial ligations, there is a relative advantage of the double- versus single-ligation approach.^{28,45} The 3D volumetric analysis provides high-resolution assessments of CHST volume that will be useful in precisely evaluating the effect of treatment with oHSV on CHST growth and the resultant osteolytic and osteoblastic processes in future experiments.

While numerous viruses have been used for OV, we chose an attenuated HSV-1 mutant due to our prior experience with this virus in the intracranial compartment. HSV-1 has 89 genes and is a 152 kb, double-stranded DNA virus. It is a neurotropic virus, which may make it particularly useful for cancers of neural origin, but it can still be used for a variety of other tumors.¹⁵ Approximately 30 kb of the HSV genome is nonessential; thus, foreign DNA can be included without affecting the ability of the virus to replicate, particularly in tumor cells. These vectors can be genetically engineered and express numerous foreign transgenes which are shown to preferentially replicate and spread in tumor cells.⁴ In addition, from a safety standpoint, readily available antivirals (eg, valacyclovir, acyclovir, vidarabine, or foscarnet) can be used to eradicate the mutant HSV if there is any concern about toxicity in the host.¹⁵ Fortunately, these viruses are attenuated; thus, antivirals have never been needed in the hundreds of patients treated to date in clinical trial or following TVEC approval.

In the current study, we have shown CHST volume reduction of up to 77% as well as reversal of both osteolytic and osteoblastic effects after treatment with oHSV. We suspect that oHSV selectively infected and replicated in CHST cells, resulting in CHST cell lysis. However, the true mechanism is currently unknown and requires further study and evaluation. Prior research from our labs has shown the ability of oHSV to preferentially eradicate CHST in vitro as opposed to control cells.²⁵ We hypothesize that oHSV replicates efficiently in

CHST cells and increases intracellular cytotoxicity, which results in the destruction of CHST cells.

One advantage of oncolytic viruses is their ability to replicate selectively within tumor tissue, thereby amplifying the initial dose. Indeed, we observed substantial reduction in CHST volume after the first oHSV treatment. This may be related both to inherent oHSV lytic activity and cytotoxicity as well as to immunomodulation. Humoral and cellular immune responses are involved that not only help eradicate CHST cells infected by oHSV, but also uninfected CHST cells (also known as a bystander effect). The four overlapping mechanisms of CHST and tumor cell death by OV are presumed to be: 1) direct cellular lysis, 2) cytokine and chemokine-induced apoptosis, 3) innate immune cell cytotoxicity, and 4) adaptive antigen-specific, T-cell antitumor responses. All of these mechanisms depend on the tumor microenvironment. The goal is to maximize the therapeutic effects of OV and minimize the side effects. A greater knowledge about CHST biology will allow us to better understand the direct and indirect components and actions of OV. There are also numerous differences in mechanisms of action between different viruses as well as differences between different tumor types and different animals tested.¹⁰ Thus, the mechanisms above may vary with a human CHST as opposed to a gerbil CHST.

Failure of oHSV and in general, OV, can be due to a variety of reasons: 1) host antiviral responses from the immune system; 2) tumor type variability; and 3) tumor microenvironment. Susceptibility to oHSV infection correlates with the expression of the HSV receptor on host cells. As further research is performed, our group will assess the maximum efficacy of this treatment (eg, volume of CHST tissue in which this therapy would not work well) as well as whether it needs to be combined with other therapy, such as antibacterial agents, which could reduce the concurrent biofilm formation and infection. These further steps could potentially improve the specificity and efficacy of oHSV against CHST in the future.

The limitations of this study include a relatively small number of animals. In future studies, we plan to increase the number of animals evaluated, particularly to determine the mechanism of action of oHSV against CHST. Debulking of CHST lesions (as would occur in the operating room) followed by oHSV treatment may improve the impact of OV on CHST. This was not addressed in our current study. In addition, while we have preliminary, pilot efficacy data (ie, we chose to focus on efficacy before safety), we have limited data on safety and neurotoxicity. The goal is to use lytic viruses to destroy CHST while avoiding damage to normal cells, such as those of the facial nerve, the auditory and vestibular systems, and neurovascular tissue.¹⁰ We plan to assess for signs of involvement of neurovascular tissues (eg, histopathologic specimens of the facial nerve and brain tissue adjacent to the bulla as well as normal middle ear mucosa and normal epithelial cell of the EAC and TM). We also plan to monitor auditory function via bone-conduction auditory brainstem response measures. Acoustic stimulation via bone conduction is needed to bypass

the conductive attenuation of the ear canal ligation and presence of the CHST. Vestibular function will also be assessed through gait analysis in future studies.

Another limitation of the study is the use of micro-CT to assess bullar involvement by CHST. It is possible that some of what is noted on the scan is actually concomitant infection or effusion and not all CHST, as noted in the gross pathologic evaluation of the bullar specimens (Table II). Future studies will include the use of diffusion-weighted imaging magnetic resonance imaging scans to better assess intrabullar contents.

CONCLUSION

An OV, in this case oHSV, has been shown to have significant effect on the destruction of CHST in an in vivo gerbil model. oHSV treatment reduced CHST volume by as much as 77% with as little as one injection. Further in vivo research will be needed to elucidate if and when this treatment is most effective as well as safe. The ultimate goal is to proceed to a human clinical trial, with the goal of developing a biologic cure for CHST. Particularly after surgery, oHSV could provide the first minimally invasive, postsurgical adjuvant therapy for CHST to minimize the risk of recurrence, a potentially novel and revolutionary modality in the treatment of CHST.

Acknowledgments

The authors wish to thank the following individuals for their assistance with this project: Lisa Lemen, PhD, and Sharon Wang, MS (microCT image acquisition); Joseph Pinkl, AuD, Jennifer Gale, BS, Lindsey Bittinger, BS, Kara Kerns, BS, Randi Wray, BS (data analysis); Mary Kemper (manuscript review).

BIBLIOGRAPHY

- Soldati D, Mudry A. Knowledge about cholesteatoma, from the first description to the modern histopathology. *Otol Neurotol* 2001;22(6):723–730.
- Hamed MA, Nakata S, Sayed RH, et al. Pathogenesis and bone resorption in acquired cholesteatoma: current knowledge and future prospectives. *Clin Exp Otorhinolaryngol* 2016;9(4):298–308.
- Kemppainen HO, Puhakka HJ, Laippala PJ, Sipila MM, Manninen MP, Karma PH. Epidemiology and aetiology of middle ear cholesteatoma. *Acta Otolaryngol* 1999;119(5):568–572.
- Prasad SC, La Melia C, Medina M, et al. Long-term surgical and functional outcomes of the intact canal wall technique for middle ear cholesteatoma in the paediatric population. *Acta Otorhinolaryngol Ital* 2014;34(5):354–361.
- Kalcioglu MT, Guldemir D, Unaldi O, Egilmez OK, Celebi B, Durmaz R. Meta-genomics analysis of bacterial population of tympanosclerotic plaques and cholesteatomas. *Otolaryngol Head Neck Surg* 2018;159(4):724–732.
- Kuo CL. Etiopathogenesis of acquired cholesteatoma: prominent theories and recent advances in biomolecular research. *Laryngoscope* 2015;125(1):234–240.
- Lin E, Nemunaitis J. Oncolytic viral therapies. *Cancer Gene Ther* 2004;11(10):643–664.
- Fukuhara H, Ino Y, Todo T. Oncolytic virus therapy: a new era of cancer treatment at dawn. *Cancer Sci* 2016;107(10):1373–1379.
- Watanabe D, Goshima F. Oncolytic virotherapy by HSV. *Adv Exp Med Biol* 2018;1045:63–84.
- Cassady KA, Haworth KB, Jackson J, Markert JM, Cripe TP. To infection and beyond: the multi-pronged anti-cancer mechanisms of oncolytic viruses. *Viruses* 2016;8(2).
- Levaditi C, Nicolau S. Affinite du virus herpetique pour les neoplasmes epitheliaux. *CR Soc Biol* 1922;87:498–500.
- Levaditi C, Nicolau S. Sur le culture du virus vaccinal dans les neoplasmes epithelieus. *CR Soc Biol* 1922;86:928.
- Andtbacka RH, Kaufman HL, Collichio F, et al. Talimogene laherparepvec improves durable response rate in patients with advanced melanoma. *J Clin Oncol* 2015;33(25):2780–2788.

- Agarwalla PK, Aghi MK. Oncolytic herpes simplex virus engineering and preparation. *Methods Mol Biol* 2012;797:1–19.
- Friedman GK, Pressey JG, Reddy AT, Markert JM, Gillespie GY. Herpes simplex virus oncolytic therapy for pediatric malignancies. *Mol Ther* 2009;17(7):1125–1135.
- Mahler YY, Vaikunth SS, Currier MA, et al. Oncolytic HSV and erlotinib inhibit tumor growth and angiogenesis in a novel malignant peripheral nerve sheath tumor xenograft model. *Mol Ther* 2007;15(2):279–286.
- Markert JM, Medlock MD, Rabkin SD, et al. Conditionally replicating herpes simplex virus mutant, G207 for the treatment of malignant glioma: results of a phase I trial. *Gene Ther* 2000;7(10):867–874.
- Ning J, Wakimoto H. Oncolytic herpes simplex virus-based strategies: toward a breakthrough in glioblastoma therapy. *Front Microbiol* 2014;5:303.
- Papanastassiou V, Rampling R, Fraser M, et al. The potential for efficacy of the modified (ICP 34.5(-)) herpes simplex virus HSV1716 following intratumoural injection into human malignant glioma: a proof of principle study. *Gene Ther* 2002;9(6):398–406.
- Sivendran S, Pan M, Kaufman HL, Saenger Y. Herpes simplex virus oncolytic vaccine therapy in melanoma. *Expert Opin Biol Ther* 2010;10(7):1145–1153.
- Varghese S, Rabkin SD, Nielsen GP, MacGarvey U, Liu R, Martuza RL. Systemic therapy of spontaneous prostate cancer in transgenic mice with oncolytic herpes simplex viruses. *Cancer Res* 2007;67(19):9371–9379.
- Watanabe D, Goshima F, Mori I, Tamada Y, Matsumoto Y, Nishiyama Y. Oncolytic virotherapy for malignant melanoma with herpes simplex virus type 1 mutant HF10. *J Dermatol Sci* 2008;50(3):185–196.
- Wong RJ, Chan MK, Yu Z, et al. Effective intravenous therapy of murine pulmonary metastases with an oncolytic herpes virus expressing interleukin 12. *Clin Cancer Res* 2004;10(1 pt 1):251–259.
- Hammill AM, Conner J, Cripe TP. Oncolytic virotherapy reaches adolescence. *Pediatr Blood Cancer* 2010;55(7):1253–1263.
- Samy RN, Lipschitz N, Earl BR, Cripe TP. Evidence for oncolytic viral eradication of cholesteatoma in vitro. *Otolaryngol Head Neck Surg* 2019;160(5):891–893.
- Chole RA, Henry KR, McGinn MD. Cholesteatoma: spontaneous occurrence in the Mongolian gerbil *Meriones unguiculatus*. *Am J Otol* 1981;2(3):204–210.
- McGinn MD, Chole RA, Henry KR. Cholesteatoma. Experimental induction in the Mongolian Gerbil, *Meriones Unguiculus*. *Acta Otolaryngol* 1982;93(1–2):61–67.
- Jung JY, Lee DH, Wang EW, et al. *P. aeruginosa* infection increases morbidity in experimental cholesteatomas. *Laryngoscope* 2011;121(11):2449–2454.
- Oliszewska E, Wagner M, Bernal-Sprekelsen M, et al. Etiopathogenesis of cholesteatoma. *Eur Arch Otorhinolaryngol* 2004;261(1):6–24.
- Giavarina D. Understanding Bland Altman analysis. *Biochem Med* 2015;25(2):141–151.
- Subbiah V, Chuang HH, Gambhire D, Kairemo K. Defining clinical response criteria and early response criteria for precision oncology: current state-of-the-art and future perspectives. *Diagnostics* 2017;7(1).
- Martuza RL, Malick A, Markert JM, Ruffner KL, Coen DM. Experimental therapy of human glioma by means of a genetically engineered virus mutant. *Science* 1991;252(5007):854–856.
- Bauzon M, Hermiston T. Armed therapeutic viruses - a disruptive therapy on the horizon of cancer immunotherapy. *Front Immunol* 2014;5:74.
- Hermiston TW, Kuhn I. Armed therapeutic viruses: strategies and challenges to arming oncolytic viruses with therapeutic genes. *Cancer Gene Ther* 2002;9(12):1022–1035.
- Fong Y, Kim T, Bhargava A, et al. A herpes oncolytic virus can be delivered via the vasculature to produce biologic changes in human colorectal cancer. *Mol Ther* 2009;17(2):389–394.
- MacKie RM, Stewart B, Brown SM. Intralesional injection of herpes simplex virus 1716 in metastatic melanoma. *Lancet* 2001;357(9255):525–526.
- Sheridan C. Amgen announces oncolytic virus shrinks tumors. *Nat Biotechnol* 2013;31(6):471–472.
- Corrigan PA, Beaulieu C, Patel RB, Lowe DK. Talimogene laherparepvec: an oncolytic virus therapy for melanoma. *Ann Pharmacother* 2017;51(8):675–681.
- Berger G, Hawke M, Ekem JK. Bone resorption in chronic otitis media. The role of mast cells. *Acta Otolaryngol* 1985;100(1–2):72–80.
- Jung JY, Pashia ME, Nishimoto SY, Faddis BT, Chole RA. A possible role for nitric oxide in osteoclastogenesis associated with cholesteatoma. *Otol Neurotol* 2004;25(5):661–668.
- Peek FA, Huisman MA, Berckmans RJ, Sturk A, Van Loon J, Grote JJ. Lipopolysaccharide concentration and bone resorption in cholesteatoma. *Otol Neurotol* 2003;24(5):709–713.
- Kuo CL, Lien CF, Shiao AS. Mastoid obliteration for pediatric suppurative cholesteatoma: long-term safety and sustained effectiveness after 30 years' experience with cartilage obliteration. *Audiol Neurootol* 2014;19(6):358–369.
- le Nobel GJ, James AL. Recommendations for potassium-titanyl-phosphate laser in the treatment of cholesteatoma. *J Int Adv Otol* 2016;12(3):332–336.
- Park JH, Ahn J, Moon IJ. Transcanal endoscopic ear surgery for congenital cholesteatoma. *Clin Exp Otorhinolaryngol* 2018;11(4):233–241.
- Yamamoto-Fukuda T, Hishikawa Y, Shibata Y, Kobayashi T, Takahashi H, Koji T. Pathogenesis of middle ear cholesteatoma: a new model of experimentally induced cholesteatoma in Mongolian gerbils. *Am J Pathol* 2010;176(6):2602–2606.